

Integrative analysis of transcriptomic and metabolomic data via sparse canonical correlation analysis with incorporation of biological information

Sandra E. Safo, Shuzhao Li, Qi Long

Department of Biostatistics and Bioinformatics

Department of Medicine, Division of Pulmonary

Allergy and Critical Care Medicine

Emory University, Atlanta, GA

Abstract

Integrative analyses of different high dimensional data types are becoming increasingly popular. Similarly, incorporating prior functional relationships among variables in data analysis has been a topic of increasing interest as it helps elucidate underlying mechanisms among complex diseases. In this paper, the goal is to assess association between transcriptomic and metabolomic data from a Predictive Health Institute (PHI) study including healthy adults at high risk of developing cardiovascular diseases. To this end, we develop statistical methods for identifying sparse structure in canonical correlation analysis (CCA) with incorporation of biological/structural information. Our proposed methods use prior network structural information among genes and among metabolites to guide selection of relevant genes and metabolites in sparse CCA, providing insight on the molecular underpinning of cardiovascular disease. Our simulations demonstrate that the structured sparse CCA methods outperform several existing sparse CCA methods in selecting relevant genes and metabolites when structural information is informative and are robust to mis-specified structural information. Our analysis of the PHI study reveals that a number of genes and metabolic pathways including some known to be associated with cardiovascular diseases are enriched in the subset of genes and metabolites selected by our proposed approach.

Keywords: Biological information; Canonical correlation analysis; High dimension, low sample size; Integrative analysis; Sparsity; Structural information.

Corresponding Author: Sandra E. Safo; Email: ssafo@emory.edu

1 Introduction

Recent advancement in high-throughput, biomedical technologies has enabled the measurement of multiple data types in the same studies, including genomics, epigenomics, transcriptomics and metabolomics. Each of these data types provides a different snapshot of the underlying biological system, and combining multiple data types has been shown to be very valuable in investigating complex diseases. It has been demonstrated that individual components in these data are functionally structured in networks or pathways and incorporation of such structural information can improve analysis and lead to biologically more meaningful results (Li and Li, 2008; Pan et al., 2010; Chen et al., 2013). By the same token, it is desirable to jointly study the association between these data types with incorporation of available structural information for each data type, enabling us to uncover drivers that individually or in combination provide better insight about the biological mechanism. In this article, we develop new canonical correlation analysis (CCA) methods for studying the overall dependency structure between transcripts and metabolites while incorporating structural information for each data type.

1.1 The PHI Study

Our work is motivated by data from the Emory University and Georgia Tech PHI study. The PHI was established in 2005 with the goal of understanding and optimizing health focused on maintaining health rather than treating disease. The PHI data are collected from a longitudinal study of health measures in over 750 healthy employees of Emory University and Georgia Tech. We use data for 52 participants for whom gene expression and metabolomics data at baseline were available, and who were also at high risk of developing cardiovascular diseases defined by the Framingham risk scores (D’Agostino et al., 2008). The data consist of 32 females and 20 males with ages ranging from 19 to 67 years with a mean age of 47.35 years. The gene expression data consist of 38,624 probes and the metabolomic features consist of 6,009 features, where each metabolomic feature is defined by mass-to-charge ratio (m/z) and retention time and its relative concentration is captured by ion intensity (Roede et al., 2014). We pre-process the gene expression data using approaches from (Kohane et al., 2003). Specifically, we exclude genes with variance and entropy expression values that are respectively less than the 90th and 20th percentile, resulting in 1,547 genes. For the metabolomics data, we exclude features with more than 50% zeros, and use mummichog (Li et al., 2013) to annotate the m/z features. This results in 252 metabolites.

Let $n = 52$ be the common samples that have both transcriptomic and metabolomic data. We denote the transcriptomic and metabolomic data by $\mathbf{X} = (\mathbf{x}_1, \dots, \mathbf{x}_p)$ ($p =$

1,547) and $\mathbf{Y} = (\mathbf{y}_1, \dots, \mathbf{y}_q)$ ($q = 252$), respectively, where $\mathbf{x}, \mathbf{y} \in \mathfrak{R}^n$. Structural information for genes are represented by an undirected graph $\mathcal{G}_X = (C_X, E_X, W_X)$, where C_X is the set of nodes corresponding to the p transcriptomic features, $E_X = \{i \sim j\}$ is the set of edges indicating that features i and j are associated in a biologically meaningful way, and W_X includes the weight of each node. Similarly, let $\mathcal{G}_Y = (C_Y, E_Y, W_Y)$ be the structural information for metabolites. For node i in \mathbf{X} , denote by d_i^X its degree i.e., the number of nodes that are directly connected to node i and by $w_i^X = f(d_i^X)$ its weight which can depend on d_i^X . Similarly, we define d_i^Y and w_i^Y . We use $w_i^X = d_i^X$ and $w_i^Y = d_i^Y$ in all our numerical studies. In our analysis of the PHI study, we obtain the gene network information from Kyoto Encyclopedia of Genes and Genomes (KEGG) (Kanehisa et al., 2016), and the metabolomic network information from mummichog software (Li et al., 2013). In the resulting gene network, there are 1,547 genes with 479 edges in total; the distribution of d_i^X ranges from 1 to 32 with a mean of 3. In the metabolomics network, there are 252 metabolites and 190 edges in total, with each edge representing a connection between metabolites via a known metabolic reaction. The distribution of d_i^Y for the metabolomics data ranges from 1 to 13 with a mean of 3.

Our goal is to assess association between genes and metabolites with incorporation of structural information for both data types, for which, to the best of our knowledge, little work has been done in statistical literature. It is especially challenging when the number of features (p or q) greatly exceeds the sample size n as the case in the motivating PHI study, and in many biomedical omics studies.

1.2 Existing Methods

CCA was developed to find linear combinations of two sets of variables that have maximum correlation, which can help understand the overall dependency structure between these two sets of variables. However, it is well known that the classical CCA suffers from the singularity of sample covariance matrices when applied to high dimensional data; it also lacks biological interpretability especially when the number of variables is large. Extensions of CCA have been proposed to overcome these limitations. Some modifications deal with the singularity of sample covariance matrices by applying a ridge-type regularization (Vinod, 1970; Safo and Ahn, 2014), assuming sample covariance matrices are identity matrices (Witten et al., 2009; Parkhomenko et al., 2009; Chalise and Fridley, 2012), or have some structure such as sparsity, bandable or Toeplitz (Chen et al., 2013). Gao et al. (2015) considered the sample covariances to be nuisance parameters and replaced their precision matrices with pseudo-inverses. The problem of biological interpretability has been tackled by assuming some coefficients are zero, implying that those variables do not contribute to the overall association between the two sets of vari-

ables (Waaijenborg et al., 2008; Parkhomenko et al., 2009; Witten et al., 2009; Chalise and Fridley, 2012; Chen et al., 2013; Gao et al., 2015). Chalise and Fridley (2012) used the CCA algorithm of Parkhomenko et al. (2009) and compared several penalty functions such as lasso (Tibshirani, 1994), elastic net (Zou and Hastie, 2005), SCAD (Fan and Li, 2001) and hard-thresholding. They concluded that elastic net and particularly SCAD achieve maximum correlation between the canonical correlation variables with more sparse canonical vectors. To achieve sparsity on the canonical vectors, Safo and Ahn (2014) imposed a l_∞ constraint on a modified generalized eigenvalue problem arising from the CCA optimization problem while minimizing the l_1 norm of linear coefficients, which was motivated by Dantzig Selector (Candes and Tao, 2007).

Despite the success of the available sparse CCA methods, their main limitation is that they do not exploit structural information among variables that is available for biological data such as transcriptomic and metabolomic data. Using available structural information, one can gain better understanding and obtain biologically more meaningful results from CCA. This has been demonstrated in the setting of sparse regression analysis (Pan et al., 2010; Li and Li, 2008; Kim and Xing, 2013). Recently, Chen et al. (2013) incorporated phylogenetic information from the bacterial taxa in CCA to study association between nutrient intake and human gut microbiome composition. We note that our work is different from the structured sparse CCA of Chen et al. (2012). In their work, they consider functional relationships among one data type and impose a group lasso penalty on the variables. Also, they do not utilize edge information among variables within pathways, which we do in the current paper.

1.3 Our Approach

We propose two structured sparse CCA methods that impose smoothness penalties on canonical correlation vectors and also allow for incorporating structural information such as gene and metabolic pathways to guide selection of important metabolites, transcripts, and pathways.

Our work makes several contributions. First, the proposed methods enable us to conduct integrative analysis of transcriptomic and metabolic data that achieves variable selection and incorporates structural information for both data types, leading to biologically more meaningful results as evidenced in our data application. Second, we develop an efficient algorithm that can handle high dimensional problems. Third, our extensive simulations demonstrate that the performance of the proposed approach is similar to or better than several existing methods even when network structure is not informative for selection of important variables. In particular, our proposed methods offer several improvements over the recent work by Chen et al. (2013). First, our CCA formulation

comes from the generalized eigenvalue problem rather than the direct CCA optimization problem. This formulation is not only simple to understand, but it also allows us to use convex objectives and constraints in the optimization problem that can be solved by most mathematical optimization softwares. Second, we use structural information from both sets of variables as opposed to only one set of variable, which is not a trivial extension. Third, their method and most sparse CCA methods assume that sample covariance matrices are identity matrices, but we relax this assumption as it can be overly restrictive in practice. In particular, our method allows the use of sparse covariance matrices (Friedman et al., 2007; Yuan and Lin, 2007) from which the underlying structural network may be inferred.

In section 2, we present the proposed structured sparse CCA after briefly reviewing sparse CCA. In Section 3, we present the algorithms for implementing the proposed sparse CCA. In Section 4, we conduct simulation studies to assess the performance of our methods in comparison with several existing methods. In Section 5, we apply our approach to the PHI study. We conclude with some discussion remarks in Section 6.

2 Methods

Following the notation introduced in Section 1, suppose that we have two sets of random matrices, an $n \times p$ matrix $\mathbf{X} = (\mathbf{x}_1, \dots, \mathbf{x}_p)$, and an $n \times q$ matrix $\mathbf{Y} = (\mathbf{y}_1, \dots, \mathbf{y}_q)$, both of which, without generality, are standardized to have column mean 0 and variance 1. CCA (Hotelling, 1936) finds projections $\boldsymbol{\alpha} \in \mathbb{R}^p$ and $\boldsymbol{\beta} \in \mathbb{R}^q$ such that the correlation between linear combinations $\mathbf{X}\boldsymbol{\alpha}$ and $\mathbf{Y}\boldsymbol{\beta}$ is maximized. Mathematically, CCA finds vectors $\boldsymbol{\alpha}$ and $\boldsymbol{\beta}$ that solve

$$\rho = \max_{\boldsymbol{\alpha}, \boldsymbol{\beta}} \text{corr}(\mathbf{X}\boldsymbol{\alpha}, \mathbf{Y}\boldsymbol{\beta}) = \max_{\boldsymbol{\alpha}, \boldsymbol{\beta}} \frac{\boldsymbol{\alpha}^T \boldsymbol{\Sigma}_{xy} \boldsymbol{\beta}}{\sqrt{\boldsymbol{\alpha}^T \boldsymbol{\Sigma}_{xx} \boldsymbol{\alpha}} \sqrt{\boldsymbol{\beta}^T \boldsymbol{\Sigma}_{yy} \boldsymbol{\beta}}},$$

where $\boldsymbol{\Sigma}_{xx}$, $\boldsymbol{\Sigma}_{yy}$ and $\boldsymbol{\Sigma}_{xy}$ are population covariance and cross-covariance matrices. The optimization problem is equivalent to solving

$$\max_{\boldsymbol{\alpha}, \boldsymbol{\beta}} \boldsymbol{\alpha}^T \boldsymbol{\Sigma}_{xy} \boldsymbol{\beta} \quad \text{subject to} \quad \boldsymbol{\alpha}^T \boldsymbol{\Sigma}_{xx} \boldsymbol{\alpha} = 1 \quad \text{and} \quad \boldsymbol{\beta}^T \boldsymbol{\Sigma}_{yy} \boldsymbol{\beta} = 1. \quad (1)$$

Using Lagrangian multipliers and some algebra, one can show that problem (1) results in a generalized eigenvalue (GEV) problem of the form

$$\begin{bmatrix} 0 & \boldsymbol{\Sigma}_{xy} \\ \boldsymbol{\Sigma}_{yx} & 0 \end{bmatrix} \begin{bmatrix} \boldsymbol{\alpha} \\ \boldsymbol{\beta} \end{bmatrix} = \rho \begin{bmatrix} \boldsymbol{\Sigma}_{xx} & 0 \\ 0 & \boldsymbol{\Sigma}_{yy} \end{bmatrix} \begin{bmatrix} \boldsymbol{\alpha} \\ \boldsymbol{\beta} \end{bmatrix}, \quad (2)$$

which can be solved by applying the singular value decomposition (SVD) to the matrix

$$\mathbf{K} = \Sigma_{xx}^{-1/2} \Sigma_{xy} \Sigma_{yy}^{-1/2} = (\mathbf{u}_1, \dots, \mathbf{u}_k) \mathbf{D} (\mathbf{v}_1, \dots, \mathbf{v}_k)^T. \quad (3)$$

Here, k is the rank of the matrix \mathbf{K} , \mathbf{u}_j and \mathbf{v}_j , ($j = 1, \dots, k$) are the j th left and right singular vectors of \mathbf{K} , and \mathbf{D} is a diagonal matrix containing singular values λ_j of \mathbf{K} ordered from the largest to the smallest. It follows that the optimal coefficients in the linear combinations of \mathbf{X} and \mathbf{Y} are given by

$$\tilde{\boldsymbol{\alpha}}_j = \Sigma_{xx}^{-1/2} \mathbf{u}_j, \quad \tilde{\boldsymbol{\beta}}_j = \Sigma_{yy}^{-1/2} \mathbf{v}_j. \quad (4)$$

The vectors $\tilde{\boldsymbol{\alpha}}_j$ and $\tilde{\boldsymbol{\beta}}_j$ are called the j th canonical correlation vectors for \mathbf{X} and \mathbf{Y} respectively, and are nonsparse. The random variables $\mathbf{X} \tilde{\boldsymbol{\alpha}}_j$ and $\mathbf{Y} \tilde{\boldsymbol{\beta}}_j$ are known as the j th canonical correlation variables, and $\tilde{\rho}_j = \lambda_j$ is the j th canonical correlation coefficient. Thus, the optimal coefficients in the linear combination yielding maximum correlation between \mathbf{X} and \mathbf{Y} is a rank one approximation of the matrix \mathbf{K} . When data are available, one can replace the population matrices $\Sigma_{xx}^{-1/2} \Sigma_{xy} \Sigma_{yy}^{-1/2}$ by the sample versions $\mathbf{S}_{xx}^{-1/2} \mathbf{S}_{xy} \mathbf{S}_{yy}^{-1/2}$, which results in consistent estimators of $\boldsymbol{\alpha}$ and $\boldsymbol{\beta}$ for fixed dimensions p, q , and large sample size n .

When p is greater than n , regularization is desirable in order to obtain interpretable solutions to the optimization problem (1). Despite the success of the existing regularized CCA methods, their main drawbacks, when applied to the setting of our interest, include failure to take full advantage of prior biological knowledge, and reliance on the assumption that $\mathbf{S}_{xx} = \mathbf{I}$, $\mathbf{S}_{yy} = \mathbf{I}$ which can be overly restrictive. Given the network information defined in Section 1.1, we investigate two structured sparse CCA for incorporating prior biological information.

2.1 Grouped Sparse CCA

The first approach is the Grouped sparse CCA, similar in spirit with Pan et al. (2010). Utilizing the graph structure in section 1.1, we propose the following structured sparse CCA criterion that solves the GEV problem (2): for the k th ($k = 1, \dots, K$) canonical correlation vector we solve iteratively until convergence the following optimization problem

$$\begin{aligned}
\min_{\boldsymbol{\alpha}} \left\{ (1 - \eta) \sum_{i \sim j} \left(\frac{|\alpha_i|^\gamma}{w_i^X} + \frac{|\alpha_j|^\gamma}{w_j^X} \right)^{1/\gamma} + \eta \sum_{d_i^X=0} |\alpha_i| \right\} & \text{ subject to } (A) \|\mathbf{S}_{xy} \tilde{\boldsymbol{\beta}}_k - \tilde{\rho}_k \tilde{\mathbf{S}}_{xx} \boldsymbol{\alpha}\|_\infty \leq \tau_{x_1} \\
& (B) \|\tilde{\mathbf{S}}_{xx}^{-1} \mathbf{S}_{xy} \tilde{\boldsymbol{\beta}}_k - \tilde{\rho}_k \boldsymbol{\alpha}\|_\infty \leq \tau_{x_2} \\
\min_{\boldsymbol{\beta}} \left\{ (1 - \eta) \sum_{i \sim j} \left(\frac{|\beta_i|^\gamma}{w_i^Y} + \frac{|\beta_j|^\gamma}{w_j^Y} \right)^{1/\gamma} + \eta \sum_{d_i^Y=0} |\beta_i| \right\} & \text{ subject to } (A) \|\mathbf{S}_{yx} \tilde{\boldsymbol{\alpha}}_k - \tilde{\rho}_k \tilde{\mathbf{S}}_{yy} \boldsymbol{\beta}\|_\infty \leq \tau_{y_1} \\
& (B) \|\tilde{\mathbf{S}}_{yy}^{-1} \mathbf{S}_{yx} \tilde{\boldsymbol{\alpha}}_k - \tilde{\rho}_k \boldsymbol{\beta}\|_\infty \leq \tau_{y_2}
\end{aligned} \tag{5}$$

where for some random vector $\mathbf{x} \in \mathfrak{R}^p$, $\|\mathbf{x}\|_\infty$ is the l_∞ norm and is defined as $\max_i |x_i|$, $i = 1, \dots, p$, $\tau_{x_1} > 0$ and $\tau_{y_1} > 0$ are tuning parameters, $\gamma > 1$ and $0 \leq \eta < 1$ are fixed, and $\tilde{\boldsymbol{\alpha}}_k$ and $\tilde{\boldsymbol{\beta}}_k$ are the k th nonsparse canonical vectors defined in (4). As defined, (A) and (B) represent two different sets of constraints and are discussed in detail in Section 3.1. The first term in each objective function is the weighted grouped penalty (Pan et al., 2010), which induces grouped variable selection. It encourages both α_i and α_j (similarly both β_i and β_j) to be equal to zero or nonzero simultaneously, implying that two neighboring variables in a network are more likely to (or not to) participate in the same biological process simultaneously. In addition, the weight w_i^X encourages $|\alpha_i|/w_i^X = |\alpha_j|/w_j^X$ (similarly $|\beta_i|/w_i^Y = |\beta_j|/w_j^Y$) for two neighboring nodes i, j , allowing for connected features to have opposite effects. The second term in each objective function encourages variable selection of singletons that are not connected to any variable in the network. The tuning parameters τ_{x_1} or τ_{x_2} and τ_{y_1} or τ_{y_2} control the number of coefficients that are exactly zero with larger values encouraging more sparsity. The selection of τ_x and τ_y is usually data-driven, and is discussed later.

We can find $\hat{\boldsymbol{\alpha}}_k$ and $\hat{\boldsymbol{\beta}}_k$, $k \geq 2$ by solving (5) after projecting data onto the orthogonal complement of $[\hat{\boldsymbol{\alpha}}_1, \dots, \hat{\boldsymbol{\alpha}}_{k-1}]$ and $[\hat{\boldsymbol{\beta}}_1, \dots, \hat{\boldsymbol{\beta}}_{k-1}]$ respectively. In other words, we deflate data by obtaining $\mathbf{X}_{new} = \mathbf{X} \mathbf{P}_k^\perp$, where \mathbf{P}_k^\perp is the projection matrix onto the orthogonal complement of $[\hat{\boldsymbol{\alpha}}_1, \dots, \hat{\boldsymbol{\alpha}}_{k-1}]$. We obtain \mathbf{Y}_{new} similarly.

In addition, in most of the existing sparse CCA methods, \mathbf{S}_{xx} (and \mathbf{S}_{yy}) is assumed to be an identity matrix, essentially assuming that \mathbf{X} (and \mathbf{Y}) is independent. We replace this assumption with the following variance-covariance matrices in our optimization problems

$$\tilde{\mathbf{S}}_{xx} = \mathbf{S}_{xx} + \sqrt{\log p/n} \mathbf{I}, \quad \tilde{\mathbf{S}}_{yy} = \mathbf{S}_{yy} + \sqrt{\log q/n} \mathbf{I} \tag{6}$$

similar in spirit with Vinod (1970). The optimization problems in (5) are convex and can be solved with an off-the-shelf convex optimization package such as the CVX package in Matlab. We provide remarks on merits of constraints (A) and (B) in Section 3. Since

the proposed method uses the nonsparse solution $(\tilde{\boldsymbol{\alpha}}_k, \tilde{\boldsymbol{\beta}}_k, \tilde{\rho}_k)$ as the ‘initial’ values, it is possible that the effectiveness of the proposed method can be dependent on the quality of initial values. To alleviate the dependence we propose to iterate the procedure by updating the $(\tilde{\boldsymbol{\alpha}}_k, \tilde{\boldsymbol{\beta}}_k, \tilde{\rho}_k)$ with the found $(\hat{\boldsymbol{\alpha}}_k, \hat{\boldsymbol{\beta}}_k, \hat{\rho}_k)$ until convergence. Here $\hat{\rho}_k$ is the correlation coefficient between $\mathbf{X}\hat{\boldsymbol{\alpha}}_k$ and $\mathbf{Y}\hat{\boldsymbol{\beta}}_k$. Algorithm 1 below describes the procedure to obtain $\hat{\boldsymbol{\alpha}}_k$ and $\hat{\boldsymbol{\beta}}_k$, $k = 1, \dots, K$.

2.2 Fused Sparse CCA

The second structured sparse CCA is the Fused sparse CCA, similar in spirit with Tibshirani et al. (2005). Utilizing the graph structure \mathcal{G} in section 1.1, we propose the following structured sparse CCA criterion that solves the GEV problem (2): for the k th ($k = 1, \dots, K$) canonical correlation vector we solve iteratively until convergence the following optimization problem

$$\begin{aligned}
\min_{\boldsymbol{\alpha}} \left\{ (1 - \eta) \sum_{i \sim j} \left| \frac{\alpha_i}{w_i^X} - \frac{\alpha_j}{w_j^X} \right| + \eta \sum_{d_i^X=0} |\alpha_j| \right\} & \text{subject to} & (A) & \|\mathbf{S}_{xy}\tilde{\boldsymbol{\beta}}_k - \tilde{\rho}_k\tilde{\mathbf{S}}_{xx}\boldsymbol{\alpha}\|_{\infty} \leq \tau_{x_1} \\
& & (B) & \|\tilde{\mathbf{S}}_{xx}^{-1}\mathbf{S}_{xy}\tilde{\boldsymbol{\beta}}_k - \tilde{\rho}_k\boldsymbol{\alpha}\|_{\infty} \leq \tau_{x_2} \\
\min_{\boldsymbol{\beta}} \left\{ (1 - \eta) \sum_{i \sim j} \left| \frac{\beta_i}{w_i^Y} - \frac{\beta_j}{w_j^Y} \right| + \eta \sum_{d_i^Y=0} |\beta_j| \right\} & \text{subject to} & (A) & \|\mathbf{S}_{yx}\tilde{\boldsymbol{\alpha}}_k - \tilde{\rho}_k\tilde{\mathbf{S}}_{yy}\boldsymbol{\beta}\|_{\infty} \leq \tau_{y_1} \\
& & (B) & \|\tilde{\mathbf{S}}_{yy}^{-1}\mathbf{S}_{yx}\tilde{\boldsymbol{\alpha}}_k - \tilde{\rho}_k\boldsymbol{\beta}\|_{\infty} \leq \tau_{y_2}
\end{aligned} \tag{7}$$

where $\tau_{x_1} > 0$ and $\tau_{y_1} > 0$ are tuning parameters, $0 \leq \eta < 1$ is assumed fixed, and $\tilde{\boldsymbol{\alpha}}_k$ and $\tilde{\boldsymbol{\beta}}_k$ are the k th nonsparse canonical vectors defined in (4). (A) and (B) are the same two sets of constraints introduced in Section 2.1. This penalty is a combination of fused lasso penalty on variable pairs that are connected in the network and an l_1 penalty on singletons that are not connected to any other variable in the network. This penalty is similar to the network constrained penalty of Li and Li (2008), but different in a number of ways. Their penalty

$$\eta_1 \sum_j |\alpha_j| + \eta_2 \sum_{i \sim j} \left(\frac{\alpha_i}{w_i} - \frac{\alpha_j}{w_j} \right)^2$$

uses the l_2 norm and it has been shown that this does not produce sparse solutions, where sparsity refers to variables that are connected in a network. In other words, it does not encourage grouped selection of variables in the network (Pan et al., 2010). In addition, the penalty $\eta_2 \sum_{i \sim j} \left(\frac{\alpha_i}{w_i} - \frac{\alpha_j}{w_j} \right)^2$ produces a ‘‘wiggly’’ solution that is less attractive for interpretation (Tibshirani et al., 2005). On the other hand, the penalty

$(1 - \eta) \sum_{i \sim j} \left| \frac{\alpha_i}{w_i} - \frac{\alpha_j}{w_j} \right|$ gives a piecewise constant solution and can be interpreted as a simple weighted average of features that are connected in a network. Also, the additional tuning parameter η_2 introduces more computational costs when applied to CCA as done in Chen et al. (2013); it requires solving a graph-constrained regression problem with dimension $(n + p) \times p$, incurring a high computational cost for very large p , particularly if one incorporates structural information on \mathbf{Y} as well. Again, we replace \mathbf{S}_{xx} and \mathbf{S}_{yy} by $\tilde{\mathbf{S}}_{xx}$ and $\tilde{\mathbf{S}}_{yy}$ respectively.

3 Computation and Algorithms

3.1 Computations

Of the two constraints in optimization problems (5) and (7), constraint (B) is computationally motivated. Let $\hat{\boldsymbol{\alpha}}_F$ and $\hat{\boldsymbol{\beta}}_F$ be solution vectors from the structured sparse optimization with constraint (A) and let $\hat{\boldsymbol{\alpha}}_S, \hat{\boldsymbol{\beta}}_S$ be solution vectors from constraint (B). It is straightforward to show that if $\tau_{x_1} = 0, \tau_{y_1} = 0$ and $\tau_{x_2} = 0, \tau_{y_2} = 0$, then $\hat{\boldsymbol{\alpha}}_F = \hat{\boldsymbol{\alpha}}_S$ and $\hat{\boldsymbol{\beta}}_F = \hat{\boldsymbol{\beta}}_S$, that is, the solution vectors are the same. However, for $\tau_{x_1} > 0, \tau_{y_1} > 0, \tau_{x_2} > 0$ and $\tau_{y_2} > 0$, the optimization problems may yield the same objective functions but the solution vectors may not be the same, i.e., $\hat{\boldsymbol{\alpha}}_F \neq \hat{\boldsymbol{\alpha}}_S$ and $\hat{\boldsymbol{\beta}}_F \neq \hat{\boldsymbol{\beta}}_S$.

When p and q are large, the optimization problems (5) and (7) with constraint (A) are expensive to compute using the CVX package since it requires inverting \mathbf{S}_{xx} , a $p \times p$ matrix, and \mathbf{S}_{yy} , a $q \times q$ matrix, at each iteration. For constraint (B), a computationally efficient approach for very high dimensional problems is described as follows. Let

$$\begin{aligned} \mathbf{X} &= \mathbf{U}_x \mathbf{D}_x \mathbf{V}_x^T \\ &= \mathbf{R}_x \mathbf{V}_x^T \end{aligned}$$

be the SVD of \mathbf{X} , where \mathbf{V}_x is a $p \times n$ matrix of right singular vectors with orthonormal columns, \mathbf{U}_x is an $n \times n$ orthogonal matrix of left singular vectors and \mathbf{D}_x is a diagonal matrix of singular values. Hence $\mathbf{R}_x = \mathbf{U}_x \mathbf{D}_x$ is also $n \times n$. Also let

$$\begin{aligned} \mathbf{Y} &= \mathbf{U}_y \mathbf{D}_y \mathbf{V}_y^T \\ &= \mathbf{R}_y \mathbf{V}_y^T \end{aligned}$$

be the SVD of \mathbf{Y} , where \mathbf{V}_y is a $q \times n$ orthonormal matrix, \mathbf{U}_y is a $n \times n$ orthogonal matrix and \mathbf{D}_y is a diagonal matrix of singular values. Then $\mathbf{R}_y = \mathbf{U}_y \mathbf{D}_y$ is also $n \times n$.

Plugging these into $\tilde{\mathbf{S}}_{xx}^{-1}\mathbf{S}_{xy}$, and after some careful linear algebra, we obtain

$$\tilde{\mathbf{S}}_{xx}^{-1}\mathbf{S}_{xy} = (\mathbf{S}_{xx} + \sqrt{\log p/n}\mathbf{I})^{-1}\mathbf{S}_{xy} = \mathbf{V}_x(\mathbf{R}_x^T\mathbf{R}_x + \sqrt{\log p/n}\mathbf{I})^{-1}\mathbf{R}_x^T\mathbf{R}_y\mathbf{V}_y^T,$$

which requires the inversion of an $n \times n$ matrix. Similarly,

$$\tilde{\mathbf{S}}_{yy}^{-1}\mathbf{S}_{yx} = (\mathbf{S}_{yy} + \sqrt{\log q/n}\mathbf{I})^{-1}\mathbf{S}_{yx} = \mathbf{V}_y(\mathbf{R}_y^T\mathbf{R}_y + \sqrt{\log q/n}\mathbf{I})^{-1}\mathbf{R}_y^T\mathbf{R}_x\mathbf{V}_x^T.$$

The same idea can be used in (3) and (4) for the nonsparse estimates $\tilde{\boldsymbol{\alpha}}_k$ and $\tilde{\boldsymbol{\beta}}_k$ in both constraints (A) and (B) to reduce computational cost of obtaining SVD of a $p \times q$ matrix, which is expensive as $\min(p, q)$ increases.

3.2 Algorithms

We describe two algorithms for the proposed structured sparse CCA methods. The first algorithm obtains the k th canonical correlation vector for fixed tuning parameters τ_x and τ_y . The second algorithm provides a data driven approach for selecting the optimal tuning parameters.

We first normalize the columns of \mathbf{X} and \mathbf{Y} to have mean zero and unit variance. Let \mathbf{u}_k and \mathbf{v}_k be the k th left and right singular vectors of $\tilde{\mathbf{S}}_{xx}^{-1/2}\mathbf{S}_{xy}\tilde{\mathbf{S}}_{yy}^{-1/2}$, and let λ_k be the k th singular value. The approach discussed in Section 3.1 can be used here for problems with large p and/or q . For fixed positive tuning parameters τ_x and τ_y , use Algorithm 1 for the k th sparse canonical correlation vectors, $\hat{\boldsymbol{\alpha}}_k$ and $\hat{\boldsymbol{\beta}}_k$.

The tuning parameters $\tau = (\tau_x, \tau_y)$ control the model complexity and their optimal values need to be selected. We use V -fold cross validation (CV) to select τ at each iteration of Algorithm 1. The optimal tuning parameter pair is chosen by performing a grid search over the entire pre-specified set of parameter values. To further reduce computational costs, we use a cross search over the pre-specified set of parameters. For a fixed value in the τ_y set of values (we fix τ_y as the middle value of the set of values), we search over the entire space of τ_x values and select $\tau_{x_{\text{opt}}}$ that minimizes criterion (8) given τ_y . Using $\tau_{x_{\text{opt}}}$, we search the entire τ_y space and choose $\tau_{y_{\text{opt}}}$ that also minimizes criterion (8). We choose $\tau_{\text{opt}} = (\tau_{x_{\text{opt}}}, \tau_{y_{\text{opt}}})$ at each iteration in Algorithm 1 since the selected optimal pair from previous iterations may be too large and may result in a trivial solution at the subsequent iteration.

Algorithm 1 Optimization for obtaining the k th structured sparse CCA vector

- 1: **for** $k = 1, \dots, K$ **do**
- 2: Initialize with nonsparse estimates: $\tilde{\boldsymbol{\alpha}}_{k0} = \tilde{\mathbf{S}}_{xx}^{-1/2} \mathbf{u}_k$, $\tilde{\boldsymbol{\beta}}_{k0} = \tilde{\mathbf{S}}_{yy}^{-1/2} \mathbf{v}_k$ with unity l_2 norm, and $\tilde{\rho}_{k0} = \lambda_k^{1/2}$. The approach discussed in Section 3.1 can be used here for problems with large p and/or q .
- 3: **for** $t=1$ until convergence or some maximum number of iterations **do**
- 4: Solve one of the following two optimization problems using previous estimates $\hat{\boldsymbol{\alpha}}_{k(t-1)}$ and $\hat{\boldsymbol{\beta}}_{k(t-1)}$, to obtain the k th estimates $\hat{\boldsymbol{\alpha}}_{k(t)}$ and $\hat{\boldsymbol{\beta}}_{k(t)}$:

(3i) The Grouped sparse optimization problem

$$\begin{aligned}
 \min_{\boldsymbol{\alpha}} \left\{ (1-\eta) \sum_{i \sim j} \left(\frac{|\alpha_i|^\gamma}{w_i^X} + \frac{|\alpha_j|^\gamma}{w_j^X} \right)^{1/\gamma} + \eta \sum_{d_i^X=0} |\alpha_i| \right\} & \quad \text{subject to} \quad (A) \|\mathbf{S}_{xy} \hat{\boldsymbol{\beta}}_{k(t-1)} - \hat{\rho}_{k(t-1)} \tilde{\mathbf{S}}_{xx} \boldsymbol{\alpha}\|_\infty \leq \tau_{x_1} \\
 & \quad \quad \quad (B) \|\tilde{\mathbf{S}}_{xx}^{-1} \mathbf{S}_{xy} \hat{\boldsymbol{\beta}}_{k(t-1)} - \hat{\rho}_{k(t-1)} \boldsymbol{\alpha}\|_\infty \leq \tau_{x_2} \\
 \min_{\boldsymbol{\beta}} \left\{ (1-\eta) \sum_{i \sim j} \left(\frac{|\beta_i|^\gamma}{w_i^Y} + \frac{|\beta_j|^\gamma}{w_j^Y} \right)^{1/\gamma} + \eta \sum_{d_i^Y=0} |\beta_i| \right\} & \quad \text{subject to} \quad (A) \|\mathbf{S}_{yx} \hat{\boldsymbol{\alpha}}_{k(t-1)} - \hat{\rho}_{k(t-1)} \tilde{\mathbf{S}}_{yy} \boldsymbol{\beta}\|_\infty \leq \tau_{y_1} \\
 & \quad \quad \quad (B) \|\tilde{\mathbf{S}}_{yy}^{-1} \mathbf{S}_{yx} \hat{\boldsymbol{\alpha}}_{k(t-1)} - \hat{\rho}_{k(t-1)} \boldsymbol{\beta}\|_\infty \leq \tau_{y_2}
 \end{aligned}$$

(3ii) The Fused sparse optimization problem

$$\begin{aligned}
 \min_{\boldsymbol{\alpha}} \left\{ (1-\eta) \sum_{i \sim j} \left| \frac{\alpha_i}{w_i^X} - \frac{\alpha_j}{w_j^X} \right| + \eta \sum_{d_i^X=0} |\alpha_j| \right\} & \quad \text{subject to} \quad (A) \|\mathbf{S}_{xy} \hat{\boldsymbol{\beta}}_{k(t-1)} - \hat{\rho}_{k(t-1)} \tilde{\mathbf{S}}_{xx} \boldsymbol{\alpha}\|_\infty \leq \tau_{x_1} \\
 & \quad \quad \quad (B) \|\tilde{\mathbf{S}}_{xx}^{-1} \mathbf{S}_{xy} \hat{\boldsymbol{\beta}}_{k(t-1)} - \hat{\rho}_{k(t-1)} \boldsymbol{\alpha}\|_\infty \leq \tau_{x_2} \\
 \min_{\boldsymbol{\beta}} \left\{ (1-\eta) \sum_{i \sim j} \left| \frac{\beta_i}{w_i^Y} - \frac{\beta_j}{w_j^Y} \right| + \eta \sum_{d_i^Y=0} |\alpha_j| \right\} & \quad \text{subject to} \quad (A) \|\mathbf{S}_{yx} \hat{\boldsymbol{\alpha}}_{k(t-1)} - \hat{\rho}_{k(t-1)} \tilde{\mathbf{S}}_{yy} \boldsymbol{\beta}\|_\infty \leq \tau_{y_1} \\
 & \quad \quad \quad (B) \|\tilde{\mathbf{S}}_{yy}^{-1} \mathbf{S}_{yx} \hat{\boldsymbol{\alpha}}_{k(t-1)} - \hat{\rho}_{k(t-1)} \boldsymbol{\beta}\|_\infty \leq \tau_{y_2}
 \end{aligned}$$

- 5: Normalize $\hat{\boldsymbol{\alpha}}_{k(t)}$ and $\hat{\boldsymbol{\beta}}_{k(t)}$ to have unity l_2 norm and obtain the canonical correlation coefficient $\hat{\rho}_{k(t)}$.
 - 6: Update $(\tilde{\boldsymbol{\alpha}}_k, \tilde{\boldsymbol{\beta}}_k, \tilde{\rho}_k)$ with $(\hat{\boldsymbol{\alpha}}_k, \hat{\boldsymbol{\beta}}_k, \hat{\rho}_k)$.
 - 7: **end for**
 - 8: If $k \geq 2$, $k \leq \min(n-1, p, q)$, update \mathbf{X} and \mathbf{Y} by projecting them to the orthogonal complement of $[\hat{\boldsymbol{\alpha}}_1, \dots, \hat{\boldsymbol{\alpha}}_{k-1}]$ and $[\hat{\boldsymbol{\beta}}_1, \dots, \hat{\boldsymbol{\beta}}_{k-1}]$ respectively, and repeat steps 3 to 7.
 - 9: **end for**
-

Algorithm 2 V-fold CV for tuning parameter selection

Randomly group the rows of \mathbf{X} and \mathbf{Y} into V roughly equal-sized groups, denoted by $\mathbf{X}^1, \dots, \mathbf{X}^V$, and $\mathbf{Y}^1, \dots, \mathbf{Y}^V$, respectively.

2: **for** each τ_x and a fixed τ_y **do**

- (i) For $v = 1, \dots, V$, let \mathbf{X}^{-v} and \mathbf{Y}^{-v} be the data matrix leaving out \mathbf{X}^v and \mathbf{Y}^v respectively. Apply Algorithm 1 on \mathbf{X}^{-v} and \mathbf{Y}^{-v} to derive the desired number of canonical correlation vectors $\hat{\boldsymbol{\alpha}}_k^{-v}(\tau_x, \tau_y)$, and $\hat{\boldsymbol{\beta}}_k^{-v}(\tau_x, \tau_y)$, $k = 1, \dots, \min(n - 1, p, q)$.
- (ii) Project \mathbf{X}^v and \mathbf{Y}^v onto $\hat{\boldsymbol{\alpha}}_k^{-v}(\tau_x, \tau_y)$, and $\hat{\boldsymbol{\beta}}_k^{-v}(\tau_x, \tau_y)$ to obtain the testing correlation coefficients, $\hat{\rho}_{k_{test}}^v(\tau_x, \tau_y) = \text{corr}(\mathbf{X}^v \hat{\boldsymbol{\alpha}}_k^{-v}, \mathbf{Y}^v \hat{\boldsymbol{\beta}}_k^{-v})$.
- (iii) Project \mathbf{X}^{-v} and \mathbf{Y}^{-v} onto $\hat{\boldsymbol{\alpha}}_k^{-v}(\tau_x, \tau_y)$, and $\hat{\boldsymbol{\beta}}_k^{-v}(\tau_x, \tau_y)$ to obtain the training correlation coefficients, $\hat{\rho}_{k_{train}}^{-v}(\tau_x, \tau_y) = \text{corr}(\mathbf{X}^{-v} \hat{\boldsymbol{\alpha}}_k^{-v}, \mathbf{Y}^{-v} \hat{\boldsymbol{\beta}}_k^{-v})$.
- (iv) Calculate the V -fold CV score as the difference between the average training and testing absolute correlation coefficients.

$$CV(\tau_x, \tau_y) = \left| \frac{1}{V} \sum_{v=1}^V |\hat{\rho}_{k_{train}}^v(\tau_x, \tau_y)| - \frac{1}{V} \sum_{v=1}^V |\hat{\rho}_{k_{test}}^{-v}(\tau_x, \tau_y)| \right|. \quad (8)$$

- (v) Select the optimal tuning parameter τ_x as $\tau_{x_{opt}} = \min CV(\tau_x, \tau_y)$

end for

4: **for** $\tau_{x_{opt}}$ and each τ_y **do**

- (i) Repeat steps 2(i) to 2(iv)
- (ii) Select the optimal tuning parameter $\tau_{y_{opt}}$ as $\tau_{y_{opt}} = \min\{CV(\tau_{x_{opt}}, \tau_y)\}$

end for

6: Apply $\tau_{opt} = (\tau_{x_{opt}}, \tau_{y_{opt}})$ on the whole training data \mathbf{X} , \mathbf{Y} to obtain the optimal canonical vectors $\hat{\boldsymbol{\alpha}}_k$, $\hat{\boldsymbol{\beta}}_k$, and coefficients $\hat{\rho}_k$ at each iteration until convergence.

4 Simulations

We conduct simulations to assess the performance of the proposed methods in comparison with several existing sparse CCA methods.

4.1 Simulation Set-up

Two hundred Monte Carlo (MC) datasets are generated as follows. The first data type \mathbf{X} have p variables and the second data type \mathbf{Y} have q variables, all drawn on the same samples with size $n = 80$. (\mathbf{X}, \mathbf{Y}) are simulated from $\text{MVN}(\mathbf{0}, \Sigma)$ with mean $\mathbf{0}$ and covariance Σ partitioned as

$$\Sigma = \begin{pmatrix} \Sigma_{xx} & \Sigma_{xy} \\ \Sigma_{yx} & \Sigma_{yy} \end{pmatrix},$$

where Σ_{xy} is the covariance between \mathbf{X} and \mathbf{Y} , and Σ_{xx} , Σ_{yy} are respectively the covariance of \mathbf{X} and \mathbf{Y} that describe the network structure in each data type. Without loss of generality, we let the first 36 variables form the networks in \mathbf{X} and \mathbf{Y} , where within each data type there are 6 main variables, each connected to 5 variables. The resulting network has 36 variables and edges with a maximum degree of 5, and $p - 36$ and $q - 36$ singletons in \mathbf{X} and \mathbf{Y} respectively. Using the notation in Section 1.1, the graph structure is given by $\mathcal{G}_X = \mathcal{G}_Y = \{C, E, W\}$, where $C = \{i, j \in p, q\}$, $E = \{i \sim j | i, j = 1, \dots, 36\}$, and $W = \{w_i | w_i = \text{degree of node } i, i = 1, \dots, 36\}$. The network structure in each data type is captured by the covariance matrices

$$\Sigma_{xx} = \begin{pmatrix} \bar{\Sigma}_{36 \times 36} & \mathbf{0} \\ \mathbf{0} & \mathbf{I}_{p-36} \end{pmatrix}, \quad \Sigma_{yy} = \begin{pmatrix} \bar{\Sigma}_{36 \times 36} & \mathbf{0} \\ \mathbf{0} & \mathbf{I}_{q-36} \end{pmatrix},$$

where $\bar{\Sigma}$ is block diagonal with 6 blocks of size 6, between-block correlation 0 and within each block there is a 5×5 compound symmetric submatrix with correlation 0.49 describing the correlation structure of the connected variables. The correlation between a main and a connecting variable is 0.7. The covariance between \mathbf{X} and \mathbf{Y} is $\Sigma_{xy} = \rho \Sigma_{xx} \boldsymbol{\alpha} \boldsymbol{\beta}^T \Sigma_{yy}$, and $\boldsymbol{\alpha}$ and $\boldsymbol{\beta}$ are the true canonical correlation vectors and ρ is the canonical correlation coefficient.

We consider four simulation scenarios.

1. Scenario one: *All networks in \mathbf{X} are correlated with all networks in \mathbf{Y}*

In the first scenario, all 6 networks in \mathbf{X} and \mathbf{Y} are associated and contribute to the correlation between the sets of variables, while the remaining singletons do not contribute to the correlation and thus have zero coefficients.. We generate the true

canonical correlation vectors $\boldsymbol{\alpha}$ and $\boldsymbol{\beta}$ as follows

$$\left(-20, \frac{-20}{\sqrt{5}}, \dots, \frac{-20}{\sqrt{5}}, 20, \frac{20}{\sqrt{5}}, \dots, \frac{20}{\sqrt{5}}, -17, \frac{-17}{\sqrt{5}}, \dots, \frac{-17}{\sqrt{5}}, 17, \frac{17}{\sqrt{5}}, \dots, \frac{17}{\sqrt{5}}, -10, \frac{-10}{\sqrt{5}}, \dots, \frac{-10}{\sqrt{5}}, 10, \frac{10}{\sqrt{5}}, \dots, \frac{10}{\sqrt{5}}, 0, \dots, 0\right)$$

and normalize such that $\boldsymbol{\alpha}^T \boldsymbol{\Sigma}_{xx} \boldsymbol{\alpha} = 1$ and $\boldsymbol{\beta}^T \boldsymbol{\Sigma}_{yy} \boldsymbol{\beta} = 1$. The canonical correlation coefficient ρ is taken as 0.9.

2. Scenario two: *Two networks in \mathbf{X} and \mathbf{Y} are correlated*

In the second scenario, only the first 2 networks in \mathbf{X} and \mathbf{Y} contribute to the correlation structure between the sets of variables. The remaining networks and singletons do not contribute to the correlation between the two data types, even though within each data type, each network exhibit strong association between variables. The true canonical correlation vectors $\boldsymbol{\alpha}$ and $\boldsymbol{\beta}$ are generated as

$$\left(-20, \frac{-20}{\sqrt{5}}, \dots, \frac{-20}{\sqrt{5}}, 20, \frac{20}{\sqrt{5}}, \dots, \frac{20}{\sqrt{5}}, 0, \dots, 0\right)$$

and we normalize each to have $\boldsymbol{\alpha}^T \boldsymbol{\Sigma}_{xx} \boldsymbol{\alpha} = 1$ and $\boldsymbol{\beta}^T \boldsymbol{\Sigma}_{yy} \boldsymbol{\beta} = 1$. The canonical correlation ρ is again taken as 0.9.

3. Scenario three: *Two orthogonal CCA vectors in \mathbf{X} and \mathbf{Y}*

In the third scenario, there are two orthogonal canonical correlation vectors $\mathbf{A} = (\boldsymbol{\alpha}_1, \boldsymbol{\alpha}_2)$ and $\mathbf{B} = (\boldsymbol{\beta}_1, \boldsymbol{\beta}_2)$ in \mathbf{X} and \mathbf{Y} respectively that induce the correlation between \mathbf{X} and \mathbf{Y} . Specifically, there are four networks in $\boldsymbol{\alpha}_1$, which are the first 24 variables with nonzero loadings, and these are associated with the first 18 variables (or 3 networks) in $\boldsymbol{\beta}_1$. The next 12 variables, forming the remaining two networks are found in $\boldsymbol{\alpha}_2$, and these are correlated with the next 3 networks in $\boldsymbol{\beta}_2$. Then, the covariance matrix between \mathbf{X} and \mathbf{Y} is $\boldsymbol{\Sigma}_{xy} = \boldsymbol{\Sigma}_{xx} \mathbf{A} \mathbf{D} \mathbf{B}^T \boldsymbol{\Sigma}_{yy}$, where $\mathbf{D} = \text{diag}(0.9, 0.6)$ is a diagonal matrix with diagonal values being the first and second canonical correlation coefficients. We normalize the vectors

$$\begin{aligned} \boldsymbol{\alpha}_1 &= \left(-20, \frac{-20}{\sqrt{5}}, \dots, \frac{-20}{\sqrt{5}}, 20, \frac{20}{\sqrt{5}}, \dots, \frac{20}{\sqrt{5}}, -17, \frac{-17}{\sqrt{5}}, \dots, \frac{-17}{\sqrt{5}}, 17, \frac{17}{\sqrt{5}}, \dots, \frac{17}{\sqrt{5}}, 0, \dots, 0\right) \\ \boldsymbol{\alpha}_2 &= \left(0, \dots, 0, 17, \frac{17}{\sqrt{5}}, \dots, \frac{17}{\sqrt{5}}, -17, \frac{-17}{\sqrt{5}}, \dots, \frac{-17}{\sqrt{5}}, 0, \dots, 0\right) \end{aligned}$$

and

$$\begin{aligned} \boldsymbol{\beta}_1 &= \left(-20, \frac{-20}{\sqrt{5}}, \dots, \frac{-20}{\sqrt{5}}, 20, \frac{20}{\sqrt{5}}, \dots, \frac{20}{\sqrt{5}}, -17, \frac{-17}{\sqrt{5}}, \dots, \frac{-17}{\sqrt{5}}, 0, \dots, 0\right) \\ \boldsymbol{\beta}_2 &= \left(0, \dots, 0, 17, \frac{17}{\sqrt{5}}, \dots, \frac{17}{\sqrt{5}}, -10, \frac{-10}{\sqrt{5}}, \dots, \frac{-10}{\sqrt{5}}, 10, \frac{10}{\sqrt{5}}, \dots, \frac{10}{\sqrt{5}}, 0, \dots, 0\right) \end{aligned}$$

to have $\boldsymbol{\alpha}_i^T \boldsymbol{\Sigma}_{xx} \boldsymbol{\alpha}_i = 1$, $\boldsymbol{\beta}_i^T \boldsymbol{\Sigma}_{yy} \boldsymbol{\beta}_i = 1$, $i = 1, 2$, $\boldsymbol{\alpha}_1^T \boldsymbol{\Sigma}_{xx} \boldsymbol{\alpha}_2 = 0$, and $\boldsymbol{\beta}_1^T \boldsymbol{\Sigma}_{yy} \boldsymbol{\beta}_2 = 0$.

4. Scenario four: *Randomly selected features in \mathbf{X} and \mathbf{Y} are correlated*

In the fourth scenario, there are two networks and 12 variables in \mathbf{X} and \mathbf{Y} that are correlated. These two networks are the same as those in scenario two, but are randomly dispersed and are not necessarily the first 12 variables in \mathbf{X} and \mathbf{Y} . We normalize the vectors to have $\boldsymbol{\alpha}^T \boldsymbol{\Sigma}_{xx} \boldsymbol{\alpha} = 1$ and $\boldsymbol{\beta}^T \boldsymbol{\Sigma}_{yy} \boldsymbol{\beta} = 1$. The canonical correlation ρ is taken as 0.9. This setting assesses performance in cases where the structural information is mis-specified or uninformative and sheds light on robustness of the proposed methods.

In the analysis of each MC dataset, we fix $\eta = .5$ and set $\gamma = 2$ in the L_γ -norm penalty of the Grouped structured sparse CCA method. We consider the dimensions $(p, q) = (500, 500)$ for all scenarios. We use 5-fold cross validation to select the optimal tuning parameters from criterion 8, and then obtain $\hat{\boldsymbol{\alpha}}$ and $\hat{\boldsymbol{\beta}}$ using the entire training set.

We evaluate the proposed methods based on their ability to select relevant features while maximizing correlation between \mathbf{X} and \mathbf{Y} . The results are summarized in terms of sensitivity, specificity, and Matthew's correlation coefficient (MCC) which are defined as follows:

$$\begin{aligned} \text{Sensitivity} &= \frac{TP}{TP + FN}, \quad \text{Specificity} = \frac{TN}{TN + FP} \\ \text{MCC} &= \frac{TP \cdot TN - FP \cdot FN}{\sqrt{(TP + FN)(TN + FP)(TP + FP)(TN + FN)}}, \end{aligned}$$

where TP, FP, TN, and FN are true positives, false positives, true negatives, and false negatives, respectively. Of note, MCC lies in the interval $[-1, 1]$, with a value of 1 corresponding to selection of all signal variables and no noise variables, a perfect selection. A value of -1 implies that $FP = 1$, $FN = 1$ and $TP = 0$, $TN = 0$, and a value of 0 implies $TP = TN = FP = FN = 0.5$.

4.2 Simulation results

We denote the proposed methods, Grouped and Fused structured sparse CCA as Grouped_A, Grouped_B, and Fused_A, Fused_B with subscripts A and B respectively indicating constraints A and B in (5) and (7). We compare with the following sparse methods: sparse CCA (SCCA) (Parkhomenko et al., 2009), penalized matrix decomposition CCA (PMD) (Witten et al., 2009), sparse CCA with SCAD penalty (SCAD) (Chalise and Fridley,

2012) and sparse estimation via linear programming for CCA (SELP)(Safo and Ahn, 2014).

Figure 1 shows the sensitivity, specificity and MCC for the methods. We observe a competitive performance of the proposed methods, in particular Fused_A and Fused_B, in selecting the true signals in all but scenario four. Fused_A and Fused_B perform well in scenarios one, three and four while Grouped_A performs better in scenario four. The other sparse methods especially SCCA and SCAD tend to select a large number of noise variables, evident by the low specificity and MCC proportions in Figure 1.

For the proposed methods, it is noticeable from the sensitivity and MCC proportions that Grouped_A and Grouped_B have a suboptimal performance in scenarios one, two and three, yet these are better than the sparse methods. In scenario two, Fused_A and Fused_B select more FP than Grouped_A and Grouped_B as evidenced by the low specificity, yet they are comparable to the other sparse methods. Recall that in scenario two, only 2 networks in \mathbf{X} and \mathbf{Y} contribute to the overall correlation between \mathbf{X} and \mathbf{Y} . However, within each network, there is high correlation, causing the Fused methods to read these as signals and therefore select them, though they do not contribute to the association between \mathbf{X} and \mathbf{Y} . In scenario four, the performance of all the methods deteriorates from scenarios one to three, yet the proposed methods still outperform the other sparse methods, suggesting that the proposed methods are robust to uninformative network information.

When we compare constraints A and B for Grouped and Fused methods, we notice similar performances in terms of variable selection and MCC for both Fused_A and Fused_B, but the latter is computationally more efficient and can be used for very high dimensional problems. For the Grouped method, Grouped_A has high specificity and high MCC values (Figure 1), but Grouped_B has better sensitivity. In general, Grouped_A outperforms Grouped_B at higher computational cost. Comparing the Fused and Grouped methods, we notice that in general, the performance of the Fused method is better than the Grouped method. However, the Grouped method (specifically Grouped_A) tends to achieve better performance in terms of specificity.

The results in Figure 1 demonstrate that the structured sparse CCA methods exhibit superior performance over the other sparse methods that are considered, evidenced by their high sensitivity, high specificity and high MCC proportions. The performance of the other sparse methods is worse in scenarios one and three than in scenario two. This shows that if the features in each set of variables are interconnected in the form of networks, and if most of these networks contribute to the association between \mathbf{X} and \mathbf{Y} , the existing sparse methods encounter difficulty in selecting the important networks. On the other hand, the proposed structured sparse methods can exploit the prior biological knowledge

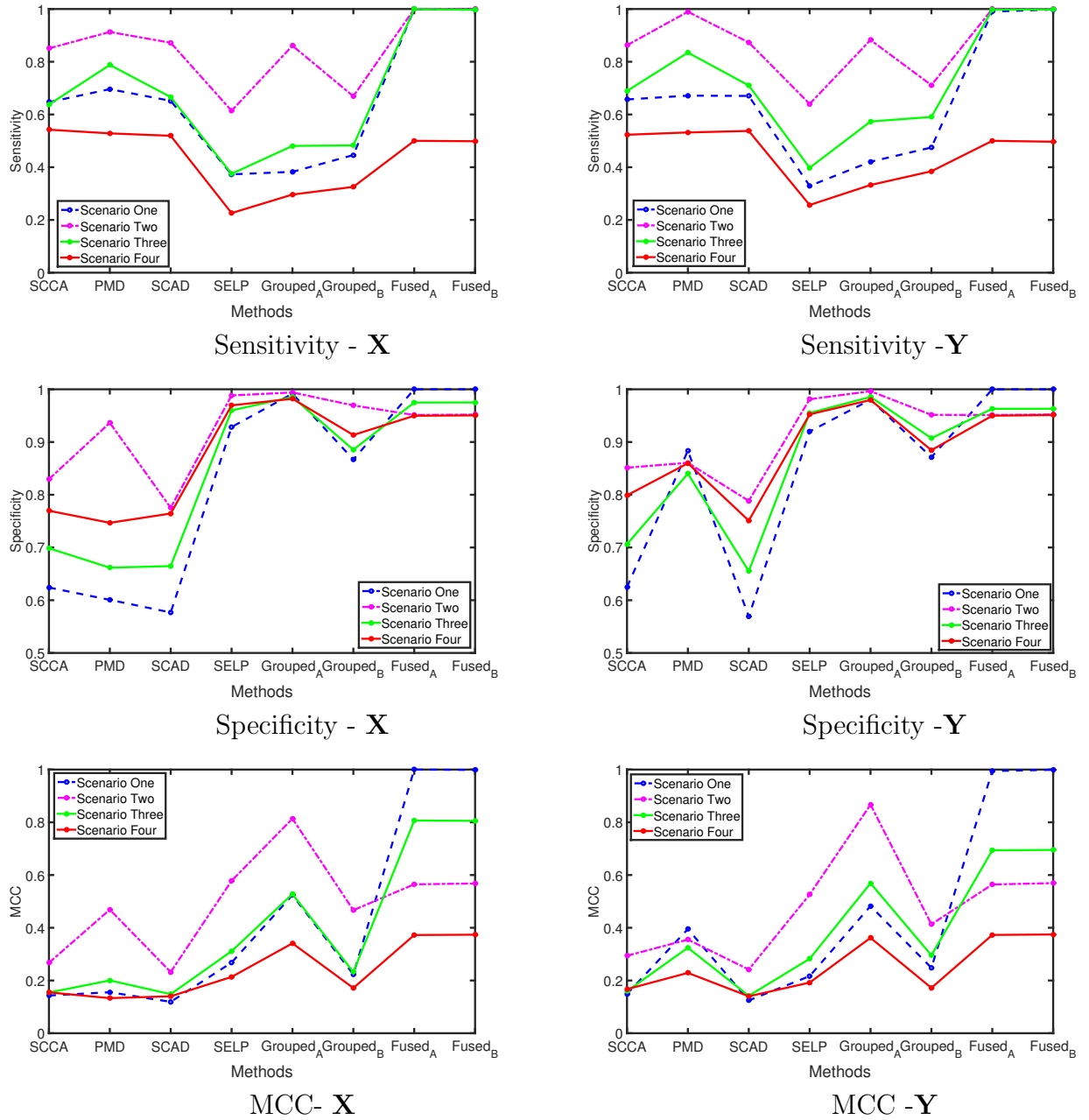


Figure 1: Comparison of structured sparse CCA with existing sparse CCA methods under scenarios one to four. MCC, Matthew's correlation coefficient.

to increase sensitivity, specificity, and MCC.

5 Analysis of the PHI Study Data

We apply the proposed methods to integrative analysis of the transcriptomic \mathbf{X} and metabolomic \mathbf{Y} data in the PHI study. We log 10 transform the metabolomics data and normalize both the transcriptomic and metabolomics data to have mean 0 and variance 1 for each transcriptomic or metabolomic feature. Our goal is to identify a subset of transcriptomic and metabolomic features that capture the overall association between transcripts and metabolites.

We apply the proposed methods and some existing sparse CCA methods to this PHI study. We use 5-fold cross validation to select optimal tuning parameters in our proposed methods, and then apply the selected tuning parameters to the whole data to estimate the maximal canonical correlation coefficient and vectors. Table 1 shows the number of genes and metabolites from the first canonical correlation vectors. Table 2 shows the number of genes and metabolites that are common among the methods. From Table 1, we observe that the proposed methods, especially Grouped_B and Fused_B have high estimated canonical correlation coefficients compared to SELP even though all select similar number of genes and metabolites. Of the proposed methods, Grouped_A is more sparse, which is consistent with the simulation results as observed by the low sensitivity and high specificity (Figure 1) when compared with Fused_A , Grouped_A , and Grouped_B . In addition, the genes and metabolites identified by Fused_A are subsets of those identified by Fused_B . It is noticeable in Table 2 that there is considerable overlap of the genes and metabolites identified by the proposed methods and the existing methods considered.

Table 1: Number of genes and metabolites selected in the first and second canonical correlation vectors in the PHI study. NA indicates that the underlying method only produce first canonical correlation vectors and coefficients.

	Genes Selected	Metabolites selected	Correlation Coefficient
	$\hat{\alpha}_1$	$\hat{\beta}_1$	$\hat{\rho}_1$
SCCA	86	154	0.7248
PMD	654	36	0.8745
SCAD	31	252	0.7036
SELP	508	152	0.8982
Grouped_A	9	4	0.8168
Grouped_B	535	137	0.9871
Fused_A	297	146	0.8658
Fused_B	536	168	0.9814

Table 2: Overlapping genes and metabolites selected in the first canonical correlation vectors in the PHI study. (\cdot, \cdot) represents number of genes and metabolites common for each pair of method compared.

	SCCA	PMD	SCAD	SELP	Grouped _A	Grouped _B	Fused _A	Fused _B
SCCA	(86,154)							
PMD	(14,20)	(654,36)						
SCAD	(31,154)	(10,36)	(31,252)					
SELP	(16,92)	(503,33)	(11,152)	(508,152)				
Grouped _A	(0,2)	(9,3)	(0,4)	(9,3)	(9,4)			
Grouped _B	(17,82)	(427,30)	(9,137)	(383,101)	(9,3)	(535,137)		
Fused _A	(13,89)	(124,24)	(4,146)	(91,91)	(2,4)	(92,77)	(297,146)	
Fused _B	(21,104)	(342,31)	(8,168)	(297,108)	(9,4)	(323,98)	(297,146)	(536,168)

We also investigate the biological relationships between the selected genes and metabolites using ToppGene Suite (Chen et al., 2009) and MetaboAnalyst 3.0 (Xia et al., 2015) respectively. These genes and metabolites are taken as input in ToppGene and MetaboAnalyst 3.0 online tools to identify pathways that are significantly enriched. The pathways that are significantly enriched in the genes selected by Fused_B include mitochondrial ATP synthesis coupled proton transport and Oxidative phosphorylation. For the metabolites, the pathways identified in Fused_B include purine and histidine metabolism. These pathways play essential roles in some important biological processes including orderly cell division, cell proliferation, differentiation and migration, and survival. For instance, cardiovascular research suggests that oxidative phosphorylation is implicated in mitochondrial dysfunction, a major factor in heart failure (Doenst et al., 2013; Rosca1 et al., 2008). In addition, several epidemiological research suggest that uric acid, which is the final end product of purine metabolism (Maiuolo et al., 2015), is an important and independent risk factor for cardiovascular diseases (Fang and Alderman, 2000; Alderman and Aiyer, 2004)

In conclusion, our analyses demonstrate that the proposed structured sparse CCA methods lead to biologically meaningful results that may shed light on the etiology of cardiovascular diseases.

6 Discussion

In this paper, we propose a new approach for integrative analysis of transcriptomic and metabolomic data. The two proposed methods, Grouped and Fused sparse CCA, allow us to not only assess association between two data types using a subset of relevant genes and metabolites, but also take into account structural information from each data type. Simulation studies demonstrate that our methods achieve better performance than several other sparse CCA methods when prior network information is informative, and

they are robust to mis-specified and uninformative network information. Applying the proposed approach to the PHI study, we show that a number of genes and metabolic pathways including some known to be associated with cardiovascular diseases are enriched in the subset of selected genes and metabolites that may shed light on the etiology of cardiovascular diseases.

Of the two methods proposed, our numerical studies show that the Fused sparse CCA performs better than the Grouped sparse CCA in terms of MCC and sensitivity, while the Grouped sparse CCA outperforms the Fused sparse CCA in terms of specificity. Our recommendation is to use the Fused sparse CCA (particularly, Fused_B) for $p \gg n$ problems, and the Grouped sparse CCA (particularly, Grouped_A) for small to moderate dimensional problems. The proposed methods are implemented in MATLAB and are available upon request. In the case where the graph information is not available, one can estimate network structures from observed data using existing approaches for sparse estimation of precision matrices (Friedman et al., 2007; Cai et al., 2011).

While our current work has focused on continuous data, it is of interest to develop similar methods for discrete data such as SNP data. When data are not continuous, CCA cannot be directly applied. To tackle this difficulty, one approach is to assume that there is a latent continuous variable for each discrete variable and use these latent variables to model the discrete variables where correlation among the latent variables is assessed using CCA. It is also of interest to extend our methods to conduct integrative analysis of more than two data types and assess nonlinear associations between multiple omics data types.

References

- Alderman, M. and Aiyer, K. J. (2004). Uric acid: role in cardiovascular disease and effects of losartan. Current Medical Research Opinion.
- Cai, T., Liu, W., and Luo, X. (2011). A constrained l_1 minimization approach to sparse precision matrix estimation. JASA Theory and Methods, 106(494):594–607.
- Candes, E. and Tao, T. (2007). The Dantzig selector: Statistical estimation when p is much larger than n . The Annals of Statistics, 35(6):2313–2351.
- Chalise, P. and Fridley, B. L. (2012). Comparison of penalty functions for sparse canonical correlation analysis. Computational Statistics and Data Analysis, 56:245–254.
- Chen, J., Bardes, E. E., Aronow, B. J., and Jegga, A. G. (2009). Toppgene suite for gene

- list enrichment analysis and candidate gene prioritization. Nucleic Acids Res, 37(Web Server issue):W305–11.
- Chen, J., Bushman, F. D., Lewis, J. D., Wu, G. D., and Li, H. (2013). Structure-constrained sparse canonical correlation analysis with an application to microbiome data analysis. Biostatistics, 14(2):244–258.
- Chen, X., Liu, H., and Carbonell, J. G. (2012). Structured sparse canonical correlation analysis. Proceedings of the 15th International Conference on Artificial Intelligence and Statistics.
- D’Agostino, R. B. S., Vasan, R. S., Pencina, M. J., Wolf, P. A., Cobain, M., Massaro, J. M., and Kannel, W. B. (2008). General cardiovascular risk profile for use in primary care: the framingham heart study. Circulation, 117(6):743–753.
- Doenst, T., Nguyen, T. D., and Abel, D. (2013). Heart failure compendium cardiac metabolism in heart failure implications beyond atp production. Circulation Research, pages 709–724.
- Fan, J. and Li, R. (2001). Variable selection via nonconcave penalized likelihood and its oracle properties. Journal of the American Statistical Association, 96(456):1348–1360.
- Fang, J. and Alderman, M. H. (2000). Serum uric acid and cardiovascular mortality the nhanes i epidemiologic follow-up study, 1971-1992. national health and nutrition examination survey. Journal of American Medical Association.
- Friedman, J., Hastie, T., and Tibshirani, R. (2007). Sparse inverse covariance estimation with graphical lasso. Biostatistics, 0(0):1–10.
- Gao, C., Ma, Z., and Zhou, H. H. (2015). Sparse cca: Adaptive estimation and computational barriers. <http://arxiv.org/pdf/1409.8565.pdf>.
- Hotelling, H. (1936). Relations between two sets of variables. Biometrika, pages 312–377.
- Kanehisa, M., Sato, Y., Kawashima, M., M, M. F., and Tanabe, M. (2016). Kegg as a reference resource for gene and protein annotation. Nucleic Acids Research, pages 457–462.
- Kim, S. and Xing, E. P. (2013). Statistical estimation of correlated genome associations to a quantitative trait network. PLOS Genetics, 5.
- Kohane, I. S., Kho, A., and Butte, A. J. (2003). Microarrays for an integrative genomics. Cambridge, MA: MIT Press.

- Li, C. and Li, H. (2008). Network-constrained regularization and variable selection for analysis of genomic data. Bioinformatics, 24(9):1175–1182.
- Li, S., Park, Y., Duraisingham, S., Strobel, H. F., Khan, N., Soltow, A. Q., and Jones, P. D. (2013). Predicting network activity from high throughput metabolomics. PLoS Comput Biol, 9(7).
- Maiuolo, J., Oppedisano, F., Gratteri, S., Muscoli, C., and Mollace, V. (2015). Regulation of uric acid metabolism and excretion. International Journal of Cardiology, pages –.
- Pan, W., Xie, B., and Shen, X. (2010). Incorporating predictor network in penalized regression. Biometrics, 66(2):474–484.
- Parkhomenko, E., Tritchler, D., and Beyene, J. (2009). Sparse canonical correlation analysis with application to genomic data integration. Statistical Applications in Genetics and Molecular Biology, 8.
- Roede, J. R., Uppal, K., Park, Y., Tran, V., and Jones, D. P. (2014). Transcriptome-metabolome wide association study (tmwas) of maneb and paraquat neurotoxicity reveals network level interactions in toxicologic mechanism. Toxicology Reports, 1:435–444.
- Rosca1, M. G., Vazquez, E. J., Kerner, J., Parland, W., Chandler, M. P., Stanley, W., Sabbah, H. N., and Hoppel, C. L. (2008). Cardiac mitochondria in heart failure: decrease in respirasomes and oxidative phosphorylation. Cardiovascular Research, 80(1):30–39.
- Safo, S. and Ahn, J. (2014). Sparse Analysis for High Dimensional Data. PhD thesis, University of Georgia.
- Tibshirani, R. (1994). Regression shrinkage and selection via the lasso. Journal of the Royal Statistical Society, Series B, 58:267–288.
- Tibshirani, R., Saunders, M., Rosset, S., Zhu, J., and Knight, K. (2005). Sparsity and smoothness via the fused lasso. Journal of the Royal Statistical Society: Series B (Statistical Methodology), 67(1):91–108.
- Vinod, H. D. (1970). Canonical ridge and econometrics of joint production. Journal of Econometrics, pages 147–166.
- Waaijenborg, S., de Witt Hamar, P. C. V., and Zwinderman, A. H. (2008). Quantifying the association between gene expressions and dna-markers by penalized canonical correlation analysis. Statistical Applications in Genetics and Molecular Biology, 7.

- Witten, D. M., Tibshirani, R. J., and Hastie, T. (2009). A penalized matrix decomposition, with applications to sparse principal components and canonical correlation analysis. Biostatistics, 10(3):515–534.
- Xia, J., Sinelnikov, I. V., Han, B., and Wishart, D. S. (2015). Metaboanalyst 3.0?making metabolomics more meaningful. Nucleic Acids Research.
- Yuan, M. and Lin, Y. (2007). Model selection and estimation in the gaussian graphical model. Biometrika, 94(1):19–35.
- Zou, H. and Hastie, T. (2005). Regularization and variable selection via the elastic net. Journal of the Royal Statistical Society, Series B, 67:301–320.